A distributed delay based controller for simultaneous periodic disturbance rejection and input-delay compensation

Can Kutlu Yuksel, Jaroslav Bušek, Milan Anderle, Tomáš Vyhlídal, Silviu-Iulian Niculescu

A Distributed Delay based Controller for Simultaneous Periodic Disturbance Rejection and Input-Delay Compensation*

Can Kutlu Yuksel[a,b], Jaroslav Bušek[a], Milan Anderle[a], Tomáš Vyhlídal [#a], Silviu-Iulian Niculescu[b]

[a] *Department of Instrumentation and Control Engineering, Faculty of Mechanical Engineering, Czech Technical University in Prague, Technická 4, Prague 6, 16607, Czechia.*
[b] *Université Paris-Saclay, CNRS, CentraleSupélec, Inria, Laboratoire des Signaux et Systèmes, 91192 Gif-sur-Yvette, France*

Abstract

The paper presents a controller design for systems suffering from multi-harmonic periodic disturbance and substantial input time-delay. It forms an alternative approach to Repetitive Control where the goal is to stabilize a close-loop that encapsulates an explicit time-delay model of the periodic signal. The proposed controller design is based on the Internal Model Control (IMC) framework, and it consists of the inverse system model and a tuneable distributed delay with an overall length related to the period of the disturbance. The properness of the controller can be ensured by utilizing a low-pass filter, however, such a component is shown to be unnecessary when the relative order of the system model is one. This fact makes the alternative approach especially suitable for systems approximated by a first-order model with input time-delay, leading to a straightforward controller design thanks to its simple structure and attainable conditions. Stability of the configuration is guaranteed by an ideal IMC framework. For further performance and robustness requirements for the non-ideal case the tuning of the controller is posed as a weighted-$\mathcal{H}_\infty$ optimization problem where frequency-, spectral- and time-domain requirements are formulated as constraints. The overall control design is experimentally verified on a laboratory setup that has high-order dynamics approximated by a first-order model with input delay.

Keywords: Periodic disturbance, time delay, internal model control, robust design

1. Introduction

Inspired by the Internal Model Principle, the repetitive control approach makes a system track/reject periodic signals by designing a controller that stabilizes the close-loop encapsulating the system and a time-delay model of the periodic signal. In this paper, the proposed control design essentially differs from that of the repetitive control by involving the model of the

*This work was supported by the Czech Science Foundation project No. 21-07321S - *Persistent problems of repetitive control*. The work of the first and fourth author was also supported by a public grant overseen by the French National Research Agency (ANR) as part of the « Investissements d'Avenir » program, through the "ADI 2020" project funded by the IDEX Paris-Saclay, ANR-11-IDEX-0003-02. The first author was also supported by the Grant Agency of the Czech Technical University in Prague, grant No. SGS23/157/OHK2/3T/12.
Corresponding author: tomas.vyhlidal@fs.cvut.cz

system in the close-loop via the Internal Model Control scheme rather than the signal model. Employing the IMC framework leads to a straightforward stability condition for the close-loop with a stable system which ideally requires only the controller to be stable and also allows us to obtain the so-called *ideal sensitivity*, which is later on subjected to a weighted-$\mathcal{H}_\infty$ optimization problem for further robustness improvements for the control. The zeros targeting the harmonic poles of the signal for tracking and rejection are placed by tuning the coefficients of a particular distributed delay employed within the controller.

For real-life applicability of the proposed control strategy, the system model employed needs to capture the original system dynamics as accurately as possible since the controller is tuned under the assumption that the *ideal setting* holds i.e. the matching between the process and its model is error-less. Fortunately, many industrial processes with high-order dynamics can be well-captured by lower-order models when associated with an input time-delay component, [1], [2], [3], [4]. Such an estimation, for instance, can be carried out using the open-loop step response of the system as in [5] and [6] or the system in close-loop arrangement as in [7]. Alternatively, the suitability of the estimated model can be determined with respect to the maximum absolute or relative error between the frequency responses of the original system and the model within a certain bandwidth. The delay component in the considered models can also directly capture the non-negligible delays arising from communication and sensor placement.

The paper mainly considers systems that can be approximated by first-order model with input time-delay of the form

$$G(s) = \frac{K}{Ts+1}\mathrm{e}^{-s\tau_m}, \tag{1}$$

with time constant T, static gain K and delay τ_m. An example of such a system is the plate thickness control in hot rolling, which practically motivates the presented research. The task is to control the vertical roll position of a hot rolling mill in order to remove the periodic surface defects caused by the inherent roll eccentricities. As it was discussed in [8, 9], the dynamic relationship between the roll position and the surface thickness can be well approximated by a first-order system with input-delay and the periodic surface defects can be treated as disturbance. The delay occurs due to the necessity of placing the sensor away from the working rolls where the actual rolling process is happening. The occurring delay is considered to be a large delay since the delay itself is greater than the time-constant of the system.

The design method presented in the paper follows an eigenvalue-based approach for time-delay systems in continuous-time. The stability of the resulting close-loop system is assessed by the spectral distribution of its characteristic roots. The periodic tracking/rejection feature is assured by the harmonic zeros placed on the imaginary axis. The robustness study is carried out in the frequency-domain and is investigated for two cases. The first case covers the robustness of the controller to inevitable process-model mismatch. It is quantified by the $\mathcal{H}_\infty$-norm of the sensitivity transfer function and is aimed to be minimized. The second case considers the robustness of the control to varying disturbance frequencies. It is quantified by the so-called *characteristic slope* κ elaborated below. The resulting distributed-delay based controller is suitable to easily implement on an industrial controller and as verified by the experimental results, executes its task overwhelmingly effective.

1.1. Repetitive Control - motivation and solutions

Repetitive control, initially introduced by Inoue [10], is a controller design to achieve periodic tracking/rejection for systems that demand such a feature. The essence of the design relies on the Internal Model Principle approach stated by Francis and Wonham [11] for linear systems: a closed-loop with a controller aimed to track/reject a particular signal must encapsulate the signal model within the loop, and the controller must have a stabilizing effect on the overall close-loop. Generalization of this principle to nonlinear systems was studied in [12] with the motivation to achieve periodic tracking/rejection by considering finitely many harmonic signal models. In the case of repetitive control, this particular signal model ideally corresponds to a time-delay model capable of representing all signals with period T_d which is given by

$$G_{\mathrm{T_d}}(s) = \frac{1}{1 - \mathrm{e}^{-sT_d}}. \tag{2}$$

However, with the time-delays occurring in the closed-loop and therefore in the characteristic equation, the overall close-loop attains an infinite-dimensional character, and assuring stability for such systems is known to be challenging. In fact, Hara et al., in [13], showed that the controller comprising the ideal model is applicable to only SISO systems with zero relative degrees and, to address this limitation, proposed the *modified repetitive control*, which is ensured to be applicable to also strictly proper systems. The proposed modification takes place in the signal model by pairing the delay with a low-pass filter $F(s)$, as in

$$G_{\mathrm{T_d}}(s) = \frac{1}{1 - F(s)\mathrm{e}^{-sT_d}}. \tag{3}$$

Figure 1 presents the scheme of this modified repetitive control which has a sensitivity transfer

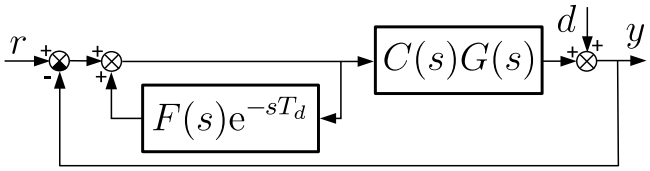

Figure 1: Repetitive Control Scheme

function expressed by

$$S(s) = \frac{1 - F(s)\mathrm{e}^{-sT_d}}{1 - F(s)\mathrm{e}^{-sT_d} + C(s)G(s)}, \tag{4}$$

where $G(s)$ and $C(s)$ denote the transfer functions of the system and the controller, respectively. Notice that the ideal case can be regained by setting $F(s) = 1$, and under this case, the transfer function has infinitely many zeros satisfying $1 - \mathrm{e}^{-sT_d} = 0$. In such a case, the zeros lie on the imaginary axis at the integer multiples of the frequency of the periodic signal generator i.e. $s_k = \mathrm{j}\frac{2\pi k}{T_d}$, $k \in \mathbb{Z}$. Since a periodic signal with a period T_d can be expressed by its Fourier series as

$$d(t) = \frac{c_0}{2} + \sum_{l=1}^{M} c_l \cos\left(\frac{2\pi l}{T_d}t - \varphi_l\right) \tag{5}$$

with $\frac{c_0}{2}$ capturing the average value of $d(t)$, $c_l, \varphi_l, l = 1, \ldots, M$ determining the amplitudes and phase shifts of the M harmonic components and M being, in general, infinite, it follows that the poles of the periodic signal model are canceled by the zeros of the sensitivity transfer function. This fact leads the error to converge to zero provided that the closed-loop is stable. However, in this ideal setting, the dynamics of the closed-loop system are described by *neutral functional differential equations* (see, e.g. [14, 15] and the references therein), having both point and essential spectrum in the linear case that make the analysis more complicated and further involved. The introduction of the low-pass filter $F(s)$ addresses this issue. Even though the filter causes the harmonic zeros to shift away from the imaginary axis, especially at high-frequencies, and, therefore, limits the precision of the signal generation, this downgrade is justified by the fact that the overall closed-loop is represented now by a set of *retarded functional differential equations* possessing only point spectrum in the linear case [14], [16]. In other words, this last setting requires less strict conditions for stabilization and later on, a stabilizing controller $C(s)$ in Fig. 1 can be found by solving a finite-dimensional stabilization problem [17].

Further on, another marking modification to improve the robustness and the non-periodic performance is the so-called *high-order repetitive control*, introduced by Inoue in [18]. In this modification, the delay in the signal model is replaced by an exponential polynomial $W(s) = \sum_{i=1}^{m} w_i \mathrm{e}^{-msT_d}$ where w_i denotes the weight of the i^{th} term, giving rise to the signal model

$$G_{\mathrm{T_d}}(s) = \frac{1}{1 - F(s)W(s)}. \tag{6}$$

The original aim discussed in [18] was to improve the non-periodic signal tracking performance of the repetitive controller by tuning the weights. Nevertheless, the degree of freedom provided by the high number of weights led to various tuning methods for objectives targeting both performance and robustness. For instance, alternative tuning methods of the weights to improve non-periodic performance [19], robustness to varying period [20] and both combined, were discussed in [21], [22]. Methods based on feed-forward and estimated disturbance-feedback schemes were studied extensively in [23].

On the other hand, alternative approaches that do not necessarily rely on the high-order repetitive controller to improve the robustness and performance do exist. In [24], robustness was studied using structured singular values. A graphical design technique that ensured the stability of the control system despite plant uncertainties was proposed in [25] and repetitive control for linear systems with time-varying and norm-bounded uncertainties was studied in [26] using Lyapunov functionals for time-delay systems. For systems with input-delay, a robust repetitive controller was designed in [27] based on μ-synthesis. For cases where the main task is to suppress disturbances, recent approaches such as those in [28, 29, 30] combine repetitive control with disturbance-observers. For nonlinear systems, an advanced form of the signal model (2) based on partial differential equation representation was employed in the design of the repetitive controller in [31]. Alternative approaches to tackle uncertain/varying frequencies based on adaptive methods were investigated in [32], [33]. Finally, repetitive consensus control for multi-agent systems was considered in [34], see also [35, 36] for cases where the multi-agent systems are subjected to stochastic disturbance and time-varying input delays.

1.2. Distributed Delays in Control and Compensation

As it will be shown, involving an IMC scheme in the periodic signal compensation provides a straightforward controller design and enables the input delay compensation. Nevertheless,

the main contribution of this paper lies in involving a *distributed delay* instead of the standard lumped delay in the harmonics compensation. This research direction builds up on the results of the broader authors team gained from the application of distributed delay in *input shaping* [37], [38], [39], [40] and *vibration absorption* using acceleration feedback [41], [42], [43]. The main benefit of using the distributed delay in input shaping, where the task is to compensate isolated modes of flexible mechanical system in a feed-forward manner, is smoothing of the command. The main benefit of involving the distributed delay in vibration suppression with acceleration feedback is in retarded spectral features at the high-frequency range. Compared to the neutral dynamics brought by the lumped delays, no further filtering is needed to save the stability at high frequencies. Note, however, that so far, the distributed delay has not been used for the periodic disturbance task considered here.

1.3. Objectives and paper outline

The objective of the proposed control design is to simplify the overall procedure to derive a controller for tracking/rejecting periodic signals and compensating input delays by exploiting the availability of an accurate yet low complexity time-delay model of the system and considering a distributed-delay structure for the controller. In contrast to the repetitive control approach, where the low-order filters introduced to achieve stability shifts the ideal zeros away from the imaginary axis, especially for high-frequencies, the proposed controller aims to place the zeros targeting the harmonics of the periodic signal exactly to their ideal location on the imaginary axis. Analytically derived conditions for the distributed delay and the posed optimization problem allow for finding such a distributed delay in a single step, contrary to the repetitive controller where the design mainly consists of two-step i.e., optimizing the signal model (6) and finding a stabilizing controller. In addition to the convenience it brings to analytical design, the chosen distributed delay structure also keeps the implementation of the controller straightforward since it can be realized similarly to a shift register-like configuration.

The paper is organised as follows. In Section 2, the IMC scheme with the main components is proposed and adjusted towards compensating both the input time delay and the periodic disturbance. The compensator design based on the distributed delay, which is the main proposition of the paper, is presented in Section 3. Section 4 presents a practically motivated case study example. Brief conclusions and further directions are highlighted in Section 5. Note that preliminary results were published in a conference paper [9]. The extension compared to [9] stems in performing the design in full complexity, paying more attention to the robust analysis and in providing extensive laboratory validation.

2. Internal Model Control and Compensation scheme

In order to fulfill the two compensation tasks (periodic disturbance and input time delay), an *Internal Model Control* (IMC) scheme is considered as shown in Fig. 2. As can be recognized, the scheme closely resembles the scheme of a Smith Predictor. However, in contrast to Smith predictor, in which stabilization of systems with delays can be carried out as if the system is delay-free, IMC yields more favorable close-loop equations for a design aimed at tracking/rejection. The IMC arrangement was first introduced and carefully studied by Garcia and Morari [44]. Its design and performance under periodic disturbances were studied in [45] and its application to first order systems with time-delay was studied by Vyhlidal and Zitek

in [46], see also [47]. Some other alternative approaches that target first-order systems with delay exposed to disturbances are the IMC-based PID tuning method and active disturbance suppression control proposed in [48] and [49], respectively.

The controlled plant in the IMC scheme in Fig. 2 is considered to be in the form

$$G(s) = \frac{y(s)}{u(s)} = G_i(s)\mathrm{e}^{-s\tau} \tag{7}$$

where u, y are the system input and output, respectively; $G_i(s)$ is assumed to be a proper and invertible transfer function, i.e. without any positive zeros, and τ is the input delay to be compensated. The transfer function $G_m(s)\mathrm{e}^{-s\tau_m}$ denotes the model of the plant with input delay τ_m. In the nominal form, it is assumed that $G_m(s) = G_i(s)$ and $\tau_m = \tau$. In this case, the

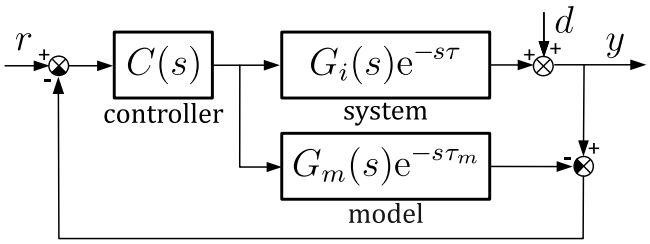

Figure 2: Proposed internal model control scheme for periodic disturbance compensation

delay τ compensation is imposed by the IMC scheme. The compensation of the multi-harmonic periodic disturbance $d(s)$ is performed by the compensator $D(s)$, which is of a distributed-delay form with an overall length T_D. The compensator output $\bar{u}$ is determined by

$$\bar{u}(t) = \int_0^{T_D} D(\eta)e(t-\eta)\,\mathrm{d}\eta \tag{8}$$

where e is the compensator input and $D(\eta)$ denotes the delay distribution. We assume the piece-wise equally distributed delay form, analogously as it was done in input shaper application [39]. In the Laplace transform form, it reads as

$$D(s) = \frac{1}{s}\sum_{k=0}^{N} a_k \mathrm{e}^{-sk\vartheta}, \tag{9}$$

where a_k are the parameters to be tuned, $\vartheta = \frac{T_D}{N}$ is the delay segment and N is the number of delay segments.

The controller $C(s)$ of the IMC scheme shown in in Fig. 2 comprises the distributed delay compensator together with the inverse model dynamic and a low-pass filter as in

$$C(s) = \frac{1}{G_m(s)}F(s)D(s), \tag{10}$$

where the low-pass filter $F(s)$ is included to guarantee that $D(s)C(s)$ is a proper (biproper, at least) transfer function, satisfying

$$\lim_{s\to 0} F(s) = 1, \tag{11}$$

i.e. having unity static gain. Considering s in the denominator of the distributed delay transfer function (9), the filter can even be omitted, i.e. $F(s) = 1$, as soon as relative degree of $G_m(s)$ is equal to one, as it is the case, e.g., for first order plus input delay system (1).

When the close-loop consists of linear subsystems, as ideally assumed for the IMC in Fig. 2, stability and tracking/rejection properties of the control system can be investigated from the poles and zeros of the sensitivity transfer function. By definition, the sensitivity function is the transfer function that relates the disturbance d to the output y, i.e., $S(s) = \frac{y(s)}{d(s)}$, [50]. The sensitivity function of the scheme in Fig. 2 is given by

$$S(s) = \frac{1 - C(s)G_m(s)\mathrm{e}^{-s\tau_m}}{1 + C(s)\left(G_i(s)\mathrm{e}^{-s\tau} - G_m(s)\mathrm{e}^{-s\tau_m}\right)}. \tag{12}$$

With the assumption $G_i(s) = G_m(s)$, $\tau = \tau_m$ and the controller in the form (10), it reduces to

$$S(s) = 1 - F(s)D(s)\mathrm{e}^{-s\tau_m}. \tag{13}$$

Note also that the ideal complementary sensitivity is given by

$$T(s) = F(s)D(s)\mathrm{e}^{-s\tau_m}. \tag{14}$$

Notice that in the nominal form (13), the input delay τ has been fully compensated and the dynamics is finite dimensional. However, this is a strong idealization and therefore, in practice, the closed loop dynamics still needs to be considered as infinite dimensional with the characteristic equation given by

$$1 + C(s)\left(G_i(s)\mathrm{e}^{-s\tau} - G_m(s)\mathrm{e}^{-s\tau_m}\right) = 0, \tag{15}$$

which can be further simplified to

$$G_m(s)\left(1 - D(s)F(s)\mathrm{e}^{-s\tau_m}\right) + D(s)F(s)G_i(s)\mathrm{e}^{-s\tau} = 0. \tag{16}$$

Taking into account that all the involved transfer functions are proper, thanks to the distributed delay features recognised in [39], the closed loop dynamics is of *retarded* time delay form with all the positive spectrum distribution features.

In cases where the interest is the close-loop robustness against delay uncertainties, the maximum delay variation $\Delta\tau := |\tau - \tau_m|$ the close-loop can tolerate, i.e., the delay margin, can be obtained utilizing geometric methods as demonstrated in [51] for Smith predictors. Note that, despite being constructed by multiple delays, the distributed delay itself is insusceptible to uncertainties in the delay values since it is fully adjustable and, once tuned, is ensured to be fixed. Therefore, it is not involved in the delay margin analysis as a source of uncertainty.

3. Shaping Delay Distribution to Compensate the Periodic Disturbance

The distributed delay $D(s)$ is to be shaped with the objective to compensate the dominant (low-frequency) harmonics of the periodic disturbance $d(t)$. Taking into account the Fourier series expansion (5), the compensation of M_d dominant harmonics with base frequency $\Omega = \frac{2\pi}{T_d}$ leads to the equation set

$$S(\mathrm{j}\Omega l) = 0, l = 1, 2, ..M_d. \tag{17}$$

By reflecting condition (17) to the nominal (ideal) sensitivity function (13) substituted with the distributed-delay (9), we get

$$\sum_{k=0}^{N} a_k \mathrm{e}^{-\mathrm{j}\Omega l k\vartheta} = \frac{\mathrm{j}\Omega l}{F(\mathrm{j}\Omega l)} \mathrm{e}^{\mathrm{j}\Omega l \tau_m}, l = 1, 2, ..M_d. \tag{18}$$

When each equation is split to its real and imaginary part, we obtain

$$\begin{aligned} \sum_{k=0}^{N} a_k \cos(\Omega l k\vartheta) &= R_l, \\ \sum_{k=0}^{N} a_k \sin(\Omega l k\vartheta) &= I_l, \end{aligned} \tag{19}$$

where

$$R_l = \Re\left(\frac{\mathrm{j}\Omega l \mathrm{e}^{\mathrm{j}\Omega l\tau_m}}{F(\mathrm{j}\Omega l)}\right), I_l = -\Im\left(\frac{\mathrm{j}\Omega l \mathrm{e}^{\mathrm{j}\Omega l\tau_m}}{F(\mathrm{j}\Omega l)}\right), \tag{20}$$

for $l = 1, 2, \ldots, M_d$.

Additional conditions to assess the coefficients a_i result from the performance and structural requirements on the compensator. Taking into account the requirements on the reference tracking and the disturbance rejection ($\lim_{s\to 0} S(s) = 0$) and considering (11), the compensator needs to have a static unity gain, i.e.

$$\lim_{s\to 0} D(s) = 1, \tag{21}$$

which is also a common requirement on the delay transfer function. For the structure in (9), this leads to the condition

$$\sum_{k=0}^{N} a_k = 0 \tag{22}$$

implying the finite impulse response feature of $D(s)$, and additionally to the condition

$$\sum_{k=0}^{N} a_k k\vartheta = -1. \tag{23}$$

Finally, the set of equations (19), (22) and (23) can be put into matrix form

$$Ax = B, \tag{24}$$

where $x \in \mathbb{R}^{N+1}$, given as $x = [a_0, a_1, ..., a_N]^{\mathrm{T}}$, $A \in \mathbb{R}^{2M_d+2\times N+1}$, $B \in \mathbb{R}^{2M_d+2}$, given as

$$A = \begin{bmatrix} 1 & \cos(\Omega\vartheta) & \cdots & \cos(\Omega N\vartheta) \\ \vdots & \vdots & \cdots & \vdots \\ 1 & \cos(\Omega M_d\vartheta) & \cdots & \cos(\Omega M_d N\vartheta) \\ 0 & \sin(\Omega\vartheta) & \cdots & \sin(\Omega N\vartheta) \\ \vdots & \vdots & \cdots & \vdots \\ 0 & \sin(\Omega M_d\vartheta) & \cdots & \sin(\Omega M_d N\vartheta) \\ 1 & 1 & \cdots & 1 \\ 0 & \vartheta & \cdots & N\vartheta \end{bmatrix}, B = \begin{bmatrix} R_1 \\ \vdots \\ R_{Md} \\ I_1 \\ \vdots \\ I_{Md} \\ 0 \\ -1 \end{bmatrix}.$$

It should be stressed that the solution of (24) requires A being of full row rank. In order to guarantee the full row rank property of A, i.e. to eliminate the potential dependencies between the rows, the periodicity in the sine and cosine functions need be avoided. This can be simply achieved by limiting the maximal difference in the trigonometric function argument in the second column of A by

$$\Omega M_d \vartheta < \pi. \tag{25}$$

Considering $\Omega = \frac{2\pi}{T_d}$ and $\vartheta = \frac{T_D}{N}$ leads us to the condition

$$2\frac{M_d}{T_d} < \frac{N}{T_D}. \tag{26}$$

The independence of values then propagates to the subsequent columns of A too. The linear independence of the last row from the others follows from trigonometric identities.

Assuming $N + 1 > M_d$, equation (24) has infinitely many solutions and can be solved via the pseudoinverse

$$x = \left(A^{\mathrm{T}}A\right)^{-1} A^{\mathrm{T}}B, \tag{27}$$

yielding the least squares solution of (24). In what follows, considering that $N + 1 \gg M_d$, we introduce additional positive features for the design of the compensator.

3.1. Optimal design

In order to enhance the closed loop robustness, we employ the standard $\mathcal{H}_\infty$-norm minimization of the weighted sensitivity function [52]. Considering the above derived conditions (24), the design is formulated as a constrained optimization problem

$$\begin{array}{ll} \min\limits_{x} & \|(1 - D(\mathrm{j}\omega)F(\mathrm{j}\omega)\mathrm{e}^{-\mathrm{j}\omega\tau_m})W(\mathrm{j}\omega)\|_\infty \ , \\ \text{s.t.} & Ax = B \\ & A_n x \leq B_n \end{array} \tag{28}$$

where

$$W(s) = \frac{\frac{1}{b_u}s + \omega_b}{s + b_l\omega_b} \tag{29}$$

is the weight function determining the desired bandwidth ω_b, lower b_l, and upper b_u bounds on the sensitivity function. The weight function helps shape the frequency response of the sensitivity function when introduced to the cost function as in (28) and ideally drives the optimization to make the sensitivity response $|S(j\omega)|$ lie under $|W^{-1}(j\omega)|$ as much as possible. This way, it becomes possible to tune the distributed delay to also account for aperiodic disturbance signals up to a certain degree determined by the stop band of $W^{-1}(s)$.

The inequality constraint in (28) can be used, e.g., to impose the limits on the jerks, i.e. maximum $J_{\max} > 0$ and minimum $J_{\min} \leq 0$ of the impulse response of $D(s)$, which results to

$$A_n = \begin{bmatrix} L \\ -L \end{bmatrix}, B_n = \begin{bmatrix} J_{\max}e_N \\ -J_{\min}e_N \end{bmatrix},$$

where $L \in \mathbb{R}^{N+1\times N+1}$ is a lower triangular matrix with $L_{p,q} = 1$, for $q \leq p$ and $L_{p,q} = 0$ otherwise, $e_N \in \mathbb{R}^{N+1}$ is the unity vector $e_N = [1, 1, \ldots, 1]^{\mathrm{T}}$. From a technical viewpoint, the

bound defined by the jerks is desired to be in its smallest possible form for two reasons. First, it indirectly helps the controller keep the instruments operating in their linear working domains. Second, it reduces the energy consumed for actuation. However, the conditions imposed for the distributed delay for tracking/rejection prevent the bound from being arbitrarily small. For instance, for the simplest case where only one zero to the origin is to be placed, conditions (22) and (23) enforce

$$\frac{1}{N\theta} < J_{max}. \tag{30}$$

Note that this distribution delay type with $J_{max} = \frac{1}{T_D}$ was studied for a distributed delay zero-vibration (ZV) input shaper designed in [40]. The lower limit on the jerk should be selected as close to zero as possible. An ideal case when $J_{min} = 0$, implying a non-decreasing character of the step response, is a standard requirement for input shapers, see e.g. [39]. Here however, due to large number of assigned zeros, the problem is likely to be unfeasible for $J_{min} = 0$.

Further observations, for instance, on condition (18), yield that the absolute sum of the coefficients is lower-bounded, i.e.

$$\Omega M_d \leq \sum_{k=0}^{N} |a_k| \,, \tag{31}$$

which in return implies that the maximum targeted frequency sets a lower limit to the bound. Nevertheless, as can be seen from these conditions, increasing the number of delay segments also benefits the bound defined through the jerks to be smaller. Therefore, the decision on the number of segments N becomes vital and must be done with respect to the emerging trade-off: higher values of N make the conditions to be satisfied easier and give flexibility for the solver; on the other hand, increased N means longer computation time and a need for a more capable controller.

Solving problem (28) relies heavily on the accuracy of the H_∞ computation and its gradient. However as stated in [53], computation of the norm for infinite dimensional systems is a rather involved task. Nevertheless, since the considered systems are SISO, the maximum of $|S(j\omega)W(j\omega)|$ within finite frequency interval can be evaluated by solving the non-linear eigenvalue problem corresponding to finding the imaginary roots $s = \mathrm{j}\omega$ of the transcendental function defined as

$$Z(s) := S_W(s)'S_W(-s) - S_W(-s)'S_W(s), \tag{32}$$

where $S_W = S(s)W(s)$, [54]. Note that, since the sensitivity is, in the case with system/model mismatch, a retarded time-delay system, the maximum of the weighted function,

$$\sup_{\omega \geq 0} |S(j\omega)W(j\omega)| \,,$$

is achieved within a finite frequency interval. In general, the H_∞ norm is a non-convex and non-smooth function with respect to the parameters [55]. Therefore, the problem in (28) needs to be handled as a constrained nonlinear optimization problem. In the application example below, the Matlab *fmincon* function is used with the initial condition resulting from (27). Alternatively, HANSO [56], (or recently designed GRANSO [57]), can be applied analogously, [55]. Note that due to the problem complexity, we cannot guarantee achieving a global minimum. Despite this fact, the locally optimal time-delay controllers can execute their tasks overwhelmingly well as soon as all the set constraints are satisfied [58].

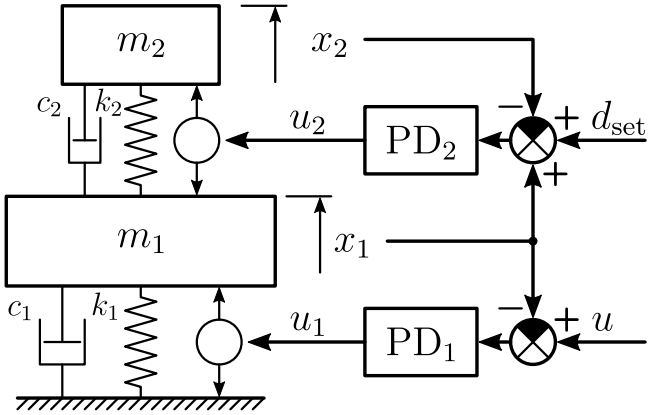

Figure 3: Scheme of the experimental set-up and inner control loops

3.2. Robustness analysis against frequency mismatch

To quantify the robustness against the frequency mismatch analogously to [41], the characteristic-slope defined as

$$\kappa(l) := \lim_{\Delta v \to +0} \frac{|S(\mathrm{j}(l\Omega + \Delta v))| - |S(\mathrm{j}(l\Omega))|}{\Delta v} = |S'(\mathrm{j}l\Omega)| \tag{33}$$

where Δv is the frequency variation, is utilized. It corresponds to the slope of the magnitude-frequency curve of the sensitivity at nominal frequency $l\Omega$ when converged from right. Hence, the smaller the slope, the lesser the sensitivity for a deviated frequency. However, one should note that, due to Bode's Sensitivity Integral, the benefit of lowering the sensitivity for some frequency intervals is paid by increased sensitivity for frequencies outside these intervals [59].

4. Experimental validation

As mentioned in the introduction, the presented research has been motivated by a hot rolling application, where a periodic disturbance and a substantial input time delay need to be compensated simultaneously. Performing the validation on an industrial rolling mill is not possible at this stage. Though, we validate the proposed method on a mechanical set-up at which we mimic the key aspects of the rolling mill application, i.e. long input delay and periodic disturbance.

The set-up is composed of two-mass system linked by the springs, dampers and actuators as shown schematically in Fig. 3. The mathematical model of the physical setup is given by

$$m_1\ddot{x}_1(t) + (c_1 + c_2)\dot{x}_1(t) + (k_1 + k_2)x_1(t) = c_2\dot{x}_2(t) + k_2x_2(t) + u_1(t) - u_2(t), \tag{34}$$

$$m_2\ddot{x}_2(t) + c_2\dot{x}_2(t) + k_2x_2(t) = c_2\dot{x}_1(t) + k_2x_1(t) + u_2(t), \tag{35}$$

where x_1, x_2 denote the positions of the bodies, and u_1, u_2 denote the control forces. The parameters m_1, m_2 denote masses of the bodies, k_1, k_2 stiffness and c_1, c_2 damping of the links. The system output to be controlled by the IMC scheme is the position of the body with m_1, i.e.

$$y(t) = x_1(t). \tag{36}$$

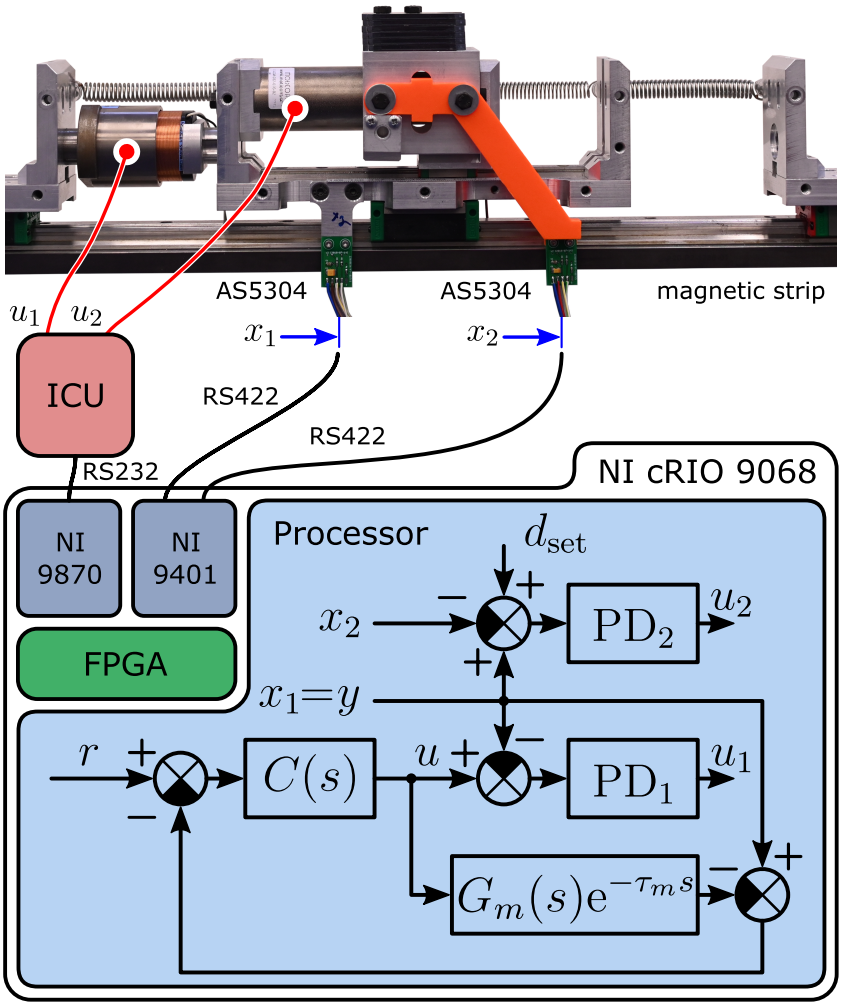

Figure 4: The mechatronic implementation of the set-up and its control system

In order to achieve dynamics described by the model (1), we introduce the inner PD control loops

$$u_1(t) = r_{o1}(u(t) - x_1(t)) - r_{d1}\dot{x}_1(t), \tag{37}$$

$$u_2(t) = r_{o2}(d_{\text{set}}(t) - \Delta x(t)) - r_{d2}\Delta\dot{x}(t), \tag{38}$$

where $\Delta x(t) = x_2(t) - x_1(t)$, u is the control input of the IMC scheme, and d_{set} is the set-point of the disturbance - the position Δx generating the disturbance force effect to the body with m_1. The parameters to be tuned to achieve non-oscillatory response in the $u \to y$ channel are the proportional r_{o1}, r_{o2} and derivative r_{d1}, r_{d2} gains.

4.1. Instrumentation and mechatronic design

The implementation of the experimental set-up depicted in Fig. 3 is shown in Fig. 4, together with implementation of the control scheme. The two carts with m_1 and m_2 are interconnected with a pair of springs. Another pair of springs is used to fix the main body cart (m_1) to the left and right base elements. Both the carts slide on rails - the m_2-cart rails are fixed to the m_1-cart while the rails of m_1-cart are fixed to the base. The carts are actuated by two voice-coil

linear motors generating forces u_1 and u_2. The damping in the cart dynamics is mainly caused by the viscous friction between the bearings and the rails. The positions x_1, x_2 of the carts are measured by incremental position sensors.

The discrete version of the proposed IMC control scheme for periodic disturbance compensation depicted in Fig. 2, obtained by zero-order hold method, was implemented in LabVIEW™ and performed using the CompactRIO controller with 1 kHz sampling. The CompactRIO controller consists of a microprocessor and an FPGA module. The microprocessor computes the nominal forces u_1 and u_2. The control action u_1 is exerted by the main control loop composed of the master IMC scheme and inner PD loop. The other control action u_2 generating the disturbance is exerted by the other PD control loop. The FPGA module is used to (i) read the quadrature incremental signals RS-422 from position sensors via digital input-output card NI9401, (ii) decoding to increment or decrement the relative positions x_1 and x_2, and (iii) to command an industrial control unit (ICU) to control voice-coil motors. Both voice-coil motors run in the force regime. The nominal value of the forces u_1 and u_2 to be applied on the movable carts is transmitted from serial card NI9870 via RS-232 into the industrial control unit. Both the reading of the quadrature signals together with its decoding and the transmission of the reference forces via RS-232 were also implemented in LabVIEW™.

4.2. Parameter Identification

In the model (34)-(35) the masses $m_1 = 1.1\,\mathrm{kg}$, $m_2 = 0.514\,\mathrm{kg}$ were obtained by weighting the carts. The stiffness coefficients $k_1 = 1750\,\mathrm{N\,m^{-1}}$, $k_2 = 407\,\mathrm{N\,m^{-1}}$, were measured utilizing the force gauge, while the damping coefficients $c_1 = 5.4\,\mathrm{N\,s\,m^{-1}}$, $c_2 = 1.8\,\mathrm{N\,s\,m^{-1}}$ were determined experimentally from a series of responses. The parameters of the PD controllers have been pre-tuned analytically by using the standard pole placement method and subsequently adjusted experimentally to obtain the well-damped response shown in Fig. 5. Consequently, the approximate model (1) parameters have been assessed as $K = 0.59$, $T = 0.018\,\mathrm{s}$ and $\tau_a = 0.012\,\mathrm{s}$. As the identified dead time approximation delay of the fourth order dynamics is relatively small, it was software-wise increased by delaying the variable $u(t-\tau)$ with $\tau = 0.2\,\mathrm{s}$. As it can be seen in Fig. 5, the model fits the measured response fairly well. Furthermore, it is easy to observe that the overall delay of the model $\tau_m = \tau + \tau_a = 0.212\,\mathrm{s}$ is substantial with respect to the time constant T. Consequently, its robust compensation by the IMC scheme is crucial to achieve favourable control system responses.

4.3. Controller and compensator design

The IMC controller is formed with respect to the identified system model (1), and in order to demonstrate its multi-harmonic suppression property. The system is exposed to an artificially created disturbance d_{set} in a form of a saw-tooth with a frequency $f = 4$ Hz, i.e. $\Omega = 25.13\,\mathrm{s^{-1}}$, determining the set-point of PD_2 controller which projects to Δx. A single period profile of this periodic signal is shown in Fig. 6, together with the coefficient c_l of its Fourier series expansion (5). As seen in its frequency domain representation, the acting disturbance consists of four dominant and several minor harmonic terms. In order to demonstrate the compensation applicability, we target eight dominant harmonics, i.e. $M_d = 8$, even though four would most likely be sufficient.

Before targeting the parameters of the distributed delay $D(s)$, turn the attention to the controller (10). As the relative degree of the considered model (1) is one, we select $F(s) = 1$.

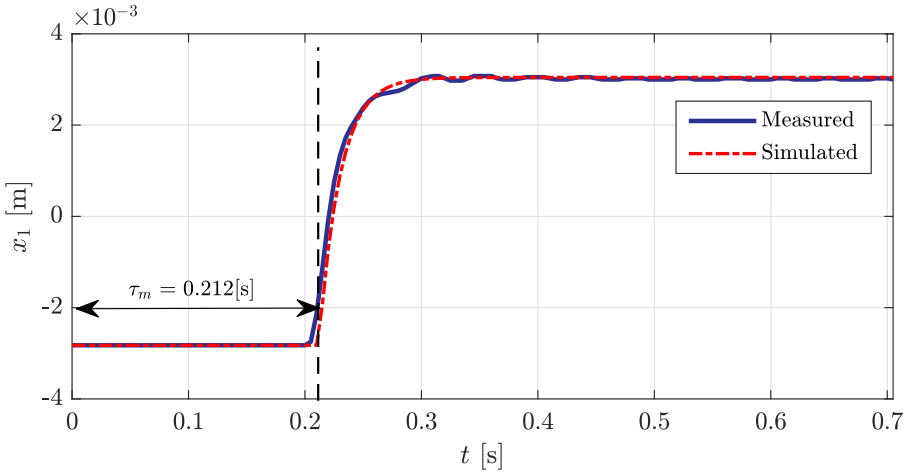

Figure 5: Transient response of the inner control loop of the set-up and its approximation by the model (1), with the visualization of the assumed input delay $\tau_m = 0.212[s]$

Then, the composed compensator-controller transfer function, which needs to be implemented at the physical controller, is given by

$$C(s) = \frac{Ts+1}{s} \sum_{k=0}^{N} a_k \mathrm{e}^{-sk\vartheta}. \tag{39}$$

The parameters for the distributed delay (9) are chosen to be $\theta = 0.01[s]$ and $N = 59$ which is in accordance with condition (26). The sufficiently large number of N provides the degrees of freedom for the optimization and is within the limits of the maximum buffer size of the industrial controller. Also, with the chosen θ value, the controller is capable of generating the control action almost in two period time of the acting disturbance. The sensitivity weight function $W(s)$ utilized in the optimization of the coefficients a_k are set to be $b_u = 1.5$, $b_l = 0.01$ and $\omega_b = 1\,\mathrm{s}^{-1}$ to provide sufficient robustness against noise and parameter mismatch. In addition, the close-loop is ensured to be insensitive to aperiodic disturbances with slow variations compared to ω_b. For the particular study, the impulse response of the distributed delay is subject to the bounds set by $J_{max} = 23$ and $J_{min} = -6$. Note that the bounds were determined so that the optimization problem (28) was feasible and the magnitude of the limits was reasonably small. Note also that the Jerk limits are set asymmetrically so that the step set-point responses are *almost* non-decreasing. Taking into account the ideal complementary sensitivity (14), for the considered $F(s) = 1$, the unit step set-point response is obtained as $y(s) = \frac{1}{s} D(s) e^{-s\tau_m}$, i.e. by integration of the $D(s)$ impulse response. However, setting $J_{min} = 0$ to impose truly non-decreasing character of the step response, makes the optimization problem (28) become unfeasible.

Solving the optimization problem (28) by *fmincon*, the results are shown in Fig. 7 - 9. The top figure in Fig. 7 shows the Bode magnitude plot of the resulting sensitivity, which is almost optimally enveloped by the inverse of the chosen weight function. The middle graph, which is a close-up view of the sensitivity at $f = 4$ Hz, shows that the characteristic slope evaluated as $\kappa = 0.5$ via (33) is in accordance with the magnitude plot and captures the local sensitivity information. Also in this graph, the provided comparison between the theoretical and actual frequency response of the experimental setup in the proximity of the base harmonic frequency

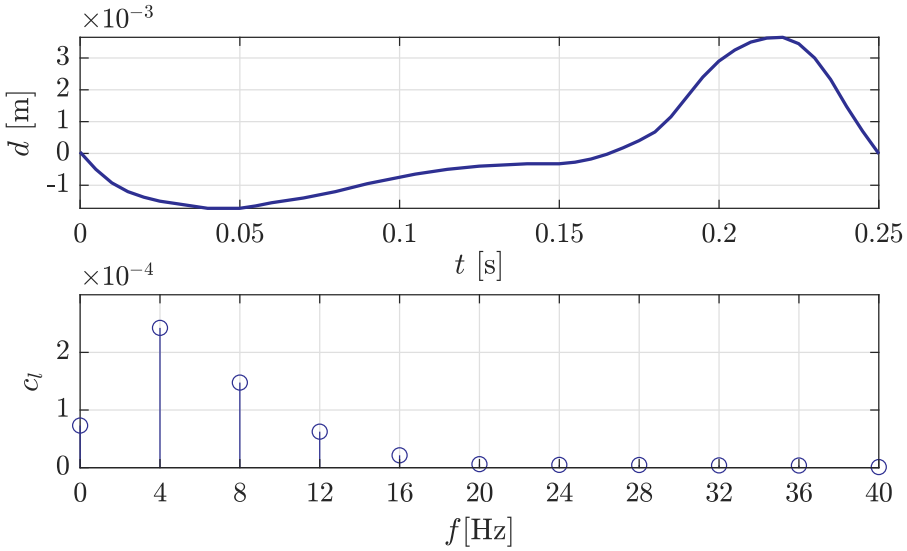

Figure 6: (**Top**) Period of the disturbance in time domain d and (**Bottom**) its frequency domain representation with magnitudes of the harmonics according to (5).

$f = 4[Hz]$ proves that the theory can precisely capture the properties of the physical system thanks to careful model parameter identification. The constraints imposed by the placement of eight harmonic zeros can be clearly seen to be satisfied in the bottom figure of Fig. 7, since the sensitivity yields zero gain at these frequencies.

The spectrum of the sensitivity (12) with the resulting optimal controller $C(s)$, approximated plant model G_m, and the fourth-order plant found as

$$G_i(s) = \frac{2286s^2 + 1.055\,10^5 s + 1.816\,10^6}{s^4 + 167.5s^3 + 9647s^2 + 2.581\,10^5 s + 3.079\,10^6}, \tag{40}$$

via (34)-(38) and $\tau = 0.2\,\mathrm{s}$ is as shown in Figure 8. Clearly, the zeros encircled in red, which are on the imaginary axis and placed at the desired positions, are another validation of the equality constraint being satisfied. Despite the obvious mismatch between the plant $G_i(s)\mathrm{e}^{-s\tau}$ and model $G_m(s)\mathrm{e}^{-s\tau_m}$, the targeted harmonic zeros are still placed correctly since the numerator of (12) is determined by G_m and τ_m only. The occurrence of pole-zero chains is due to having the numerator and the denominator of (12) in the form of a retarded quasi-polynomial when a mismatch is evident. Nevertheless, all the poles lie on the left half plane, and the controller achieves certain stability margin. As can also be seen, the high frequency poles tend to match the high frequency zeros, which results from (16).

The finite impulse response of the resulting distributed delay $D(s)$ is as shown in Fig 9. As it can be seen, the overall delay length is $T_D = \theta N = 0.59$ s and the magnitude of the N steps within the response holds the information of the evaluated coefficients a_k. Additionally, the impulse response is within limits determined by the chosen Jerk limits.

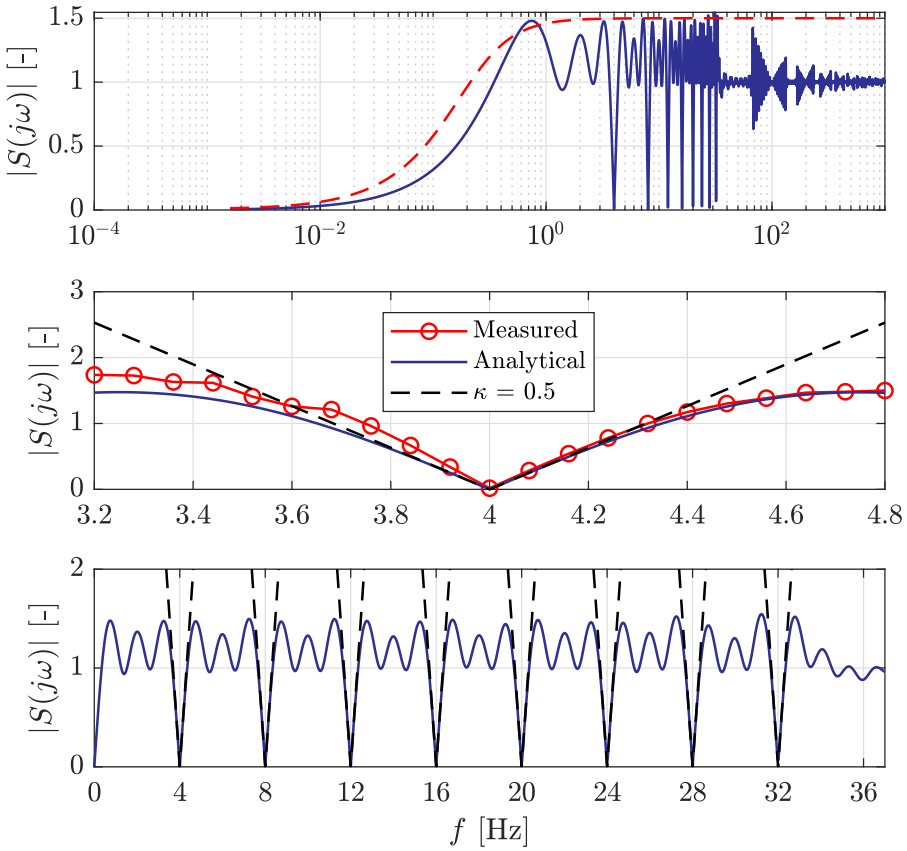

Figure 7: Amplitude responses of the sensitivity function $S(\mathrm{j}\omega)$ in frequency-domain with the considered harmonic disturbance cases (**Top**) Simulated on a large frequency range. The dashed line depicts the frequency response of $\frac{1}{W(s)}$ (**Middle**) Comparison of measured and simulated in the vicinity of the base frequency $f = 4$ [Hz]. (**Bottom**) Overall suppression performance at harmonic frequencies together with their associated characteristic slope.

4.4. Experimental validation

The proposed IMC based compensation scheme was thoroughly tested on the laboratory set-up[1]. Figure 10 shows the measured transient performance in disturbance rejection. Until $t = 2\,\mathrm{s}$, the IMC control was not active. Thus, in the region $t \in [0, 2]\mathrm{s}$, we can see the measured effect of the periodic disturbance on the system output x_1. When the IMC loop is turned on, as it can be seen, almost ideal rejection is achieved within one second with gradual suppression. All the targeted harmonics are successfully addressed up to the precision set by the sensor resolution, which is also the cause of the noisy result.

Fig. 11 shows the reference tracking performance of the IMC controller. For a practical reason, a ramp set-point change is applied. In agreement with the design, the response affected by the noise is of finite time with a duration corresponding to $\tau_m + N\vartheta + \rho = 1.002\,\mathrm{s}$, where $\rho = 0.2\,\mathrm{s}$ is the ramp signal length. Due to the ramp slope and possibly also due to filtration effect of the true fourth order dynamics, the ramp response is practically non-decreasing.

Finally, the magnitude-frequency response of the actual setup with the controller in the

[1]Video link: https://control.fs.cvut.cz/en/aclab/experiments/imcdd

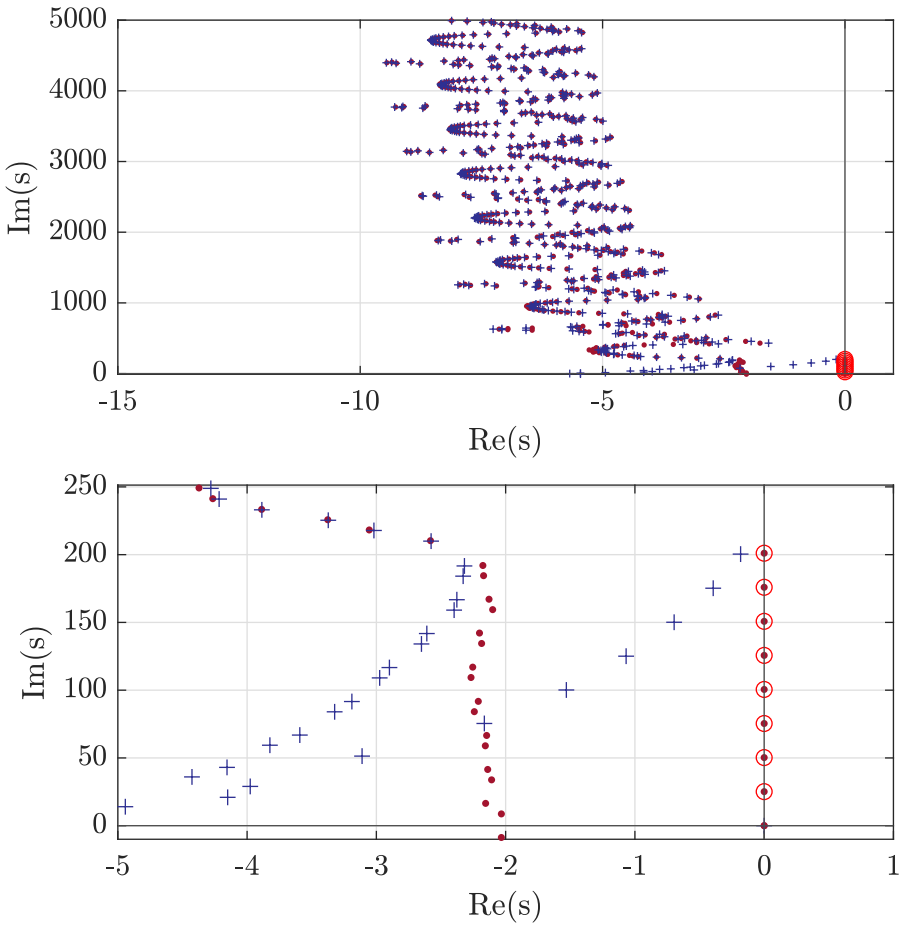

Figure 8: Pole (+) - Zero (•) spectrum of the resulting sensitivity (12) with $D(s)$, $G_m(s)$ and $G_i(s)$ given by Eq. (9) , (1) and (40), respectively. Encircled zeros correspond to the placed harmonic zeros. (**Top**) Overall distribution (**Bottom**) Close-up view on the zeros compensating the harmonics.

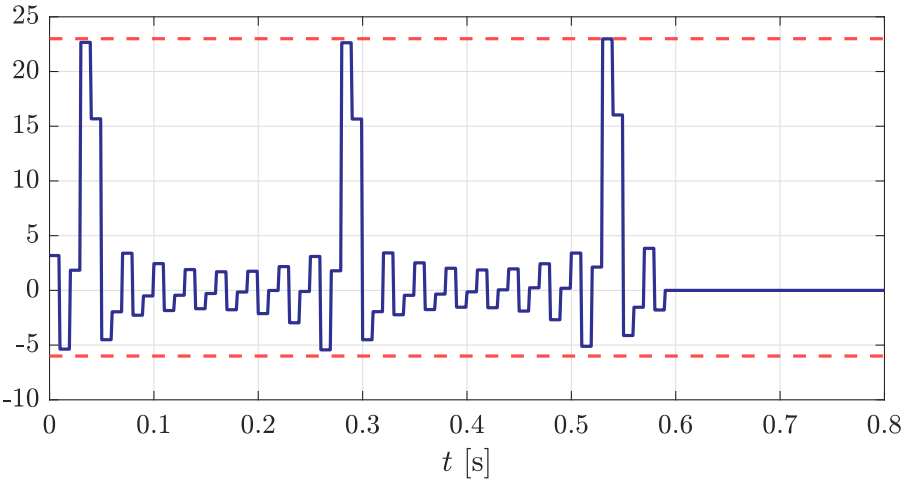

Figure 9: Impulse Response of the Optimized Distributed Delay with form (9). Dashed line - the upper ($J_{max} = 23$) and lower ($J_{min} = -6$) bounds for the Jerk.

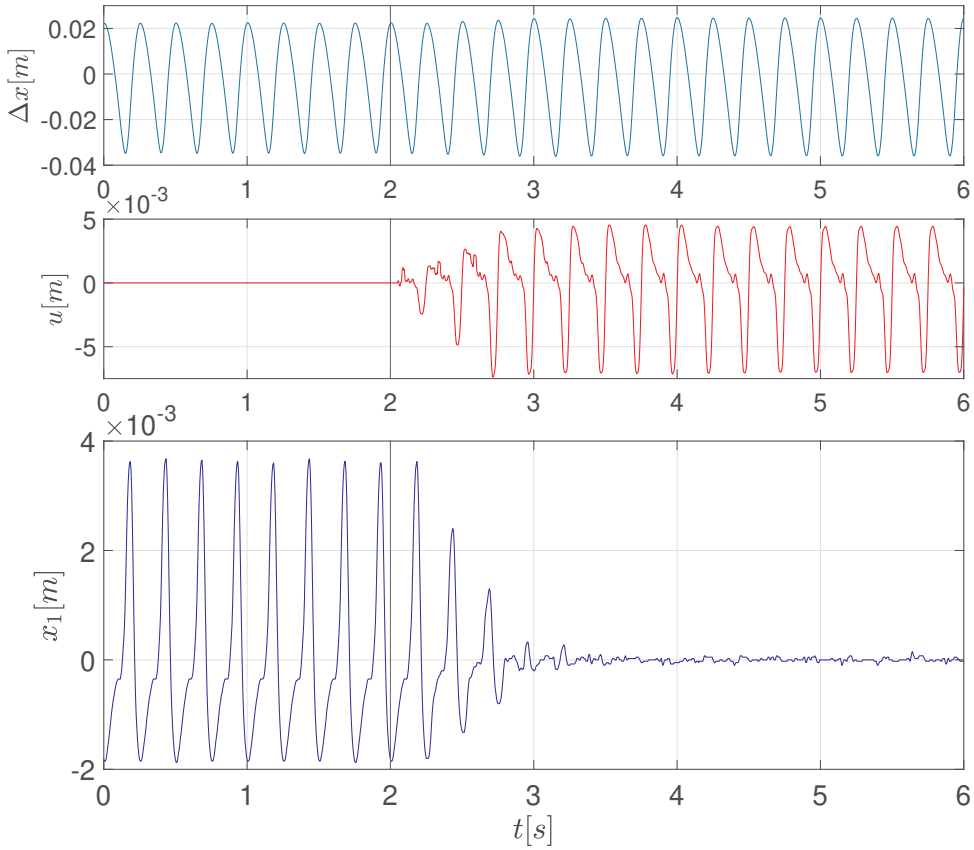

Figure 10: Experimental results for multi-harmonic disturbance compensation. The IMC loop with controller-compensator of the form (39) turned on at $t = 2s$.

vicinity of $f = 4$ [Hz] is shown in the middle graph of Fig. (7). As it can be seen, the measured response agrees with the analytically estimated one, supporting the feasibility of investigating the system with frequency-based methods.

5. Conclusion

An optimization-based control design method has been proposed for simultaneous compensation of a long input time delay and a multi-harmonic periodic disturbance. The method is directly applicable to a large class of systems and processes, which can be approximated by first order model and input time delay. Compared to the standard repetitive control, by the Internal Model Control scheme, the proposed approach was straightforward in the sense that both the controller and the compensator design are performed simultaneously. Thanks to the scheme, the delay has been compensated from the closed loop dynamics which nominally becomes of finite order. The multi-harmonic disturbance has been compensated by the multi-parameter distributed delay. The synthesis stemmed from the direct assignment of zeros at the targeted frequencies on the imaginary axis, forming the set of constraints. Thanks to the retarded spectrum brought by the distributed delay, the closed loop stability has been not endangered by the high-frequency roots. Additional constraints have been imposed by the structural properties of the distributed delay, particularly aimed at achieving its unity gain and finite impulse response.

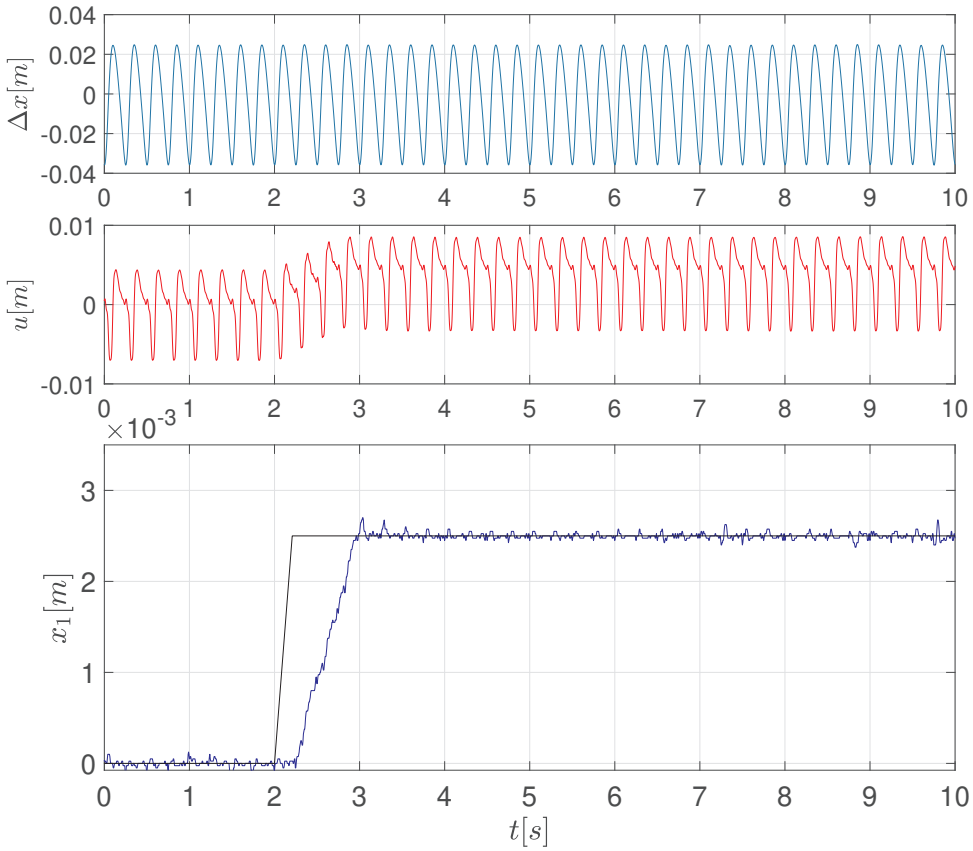

Figure 11: Experimental results for set-point response under multi-harmonic disturbance compensation, IMC loop with the controller-compensator of the form (39).

The closed loop robustness has been then obtained by minimizing the H_∞ norm of weighted sensitivity, forming the objective function of the constrained optimization problem.

The theoretical design has been thoroughly validated in an experimental case-study. The outstanding experimental results confirmed the practical applicability of the method. As demonstrated, a large number of zeros corresponding to the active harmonics can be fully and robustly covered even for a system with substantial input time delay and a certain level of plant parameter uncertainty.

Before bringing the proposed control method to an industrial application, e.g. to the referenced hot rolling problem, enhanced attention needs to be paid to online model parameter identification and to handling the nonlinearities associated with the actuator element, e.g. its saturation or rate-limit. In the subsequent research, attention will also be paid to the generalization of the proposed method to a more complex nominal model, including e.g. oscillatory modes. More attention will also be paid to the involved optimization methods with the aim to achieve a global optimum.

References

[1] B. Betlem, B. Roffel, Process dynamics and control: modeling for control and prediction, John Wiley & Sons, 2007.

[2] D. E. Seborg, T. F. Edgar, D. A. Mellichamp, F. J. Doyle III, Process dynamics and control, John Wiley & Sons, 2016.

[3] R. C. Panda, Introduction to PID controllers: theory, tuning and application to frontier areas, BoD–Books on Demand, 2012.

[4] S. Skogestad, Simple analytic rules for model reduction and pid controller tuning, Journal of process control 13 (4) (2003) 291–309.

[5] G. Fedele, A new method to estimate a first-order plus time delay model from step response, Journal of the Franklin Institute 346 (1) (2009) 1–9.

[6] T. Liu, F. Gao, A frequency domain step response identification method for continuous-time processes with time delay, Journal of Process Control 20 (7) (2010) 800–809.

[7] A. Ingimundarson, T. Hägglund, Closed-loop identification of a first-order plus dead-time model with method of moments, IFAC Proceedings Volumes 33 (10) (2000) 929–934.

[8] C. K. Yuksel, J. Busek, S.-I. Niculescu, T. Vyhlidal, Internal model controller to attenuate periodic disturbance of a first-order time-delay system, in: 2021 European Control Conference (ECC), IEEE, 2021, pp. 81–86.

[9] C. K. Yuksel, J. Busek, T. Vyhlidal, S.-I. Niculescu, M. Hromcik, Internal model control with distributed-delay-compensator to attenuate multi-harmonic periodic disturbance of time-delay system, in: 2021 60th IEEE Conference on Decision and Control (CDC), IEEE, 2021, pp. 5477–5483.

[10] T. Inoue, M. Nakano, T. Kubo, S. Matsumoto, H. Baba, High accuracy control of a proton synchrotron magnet power supply, IFAC Proceedings Volumes 14 (2) (1981) 3137–3142.

[11] B. A. Francis, W. M. Wonham, The internal model principle of control theory, Automatica 12 (5) (1976) 457–465.

[12] D. Astolfi, L. Praly, L. Marconi, Harmonic internal models for structurally robust periodic output regulation, Systems & Control Letters 161 (2022) 105154.

[13] S. Hara, Y. Yamamoto, T. Omata, M. Nakano, Repetitive control system: A new type servo system for periodic exogenous signals, IEEE Transactions on automatic control 33 (7) (1988) 659–668.

[14] J. K. Hale, S. M. V. Lunel, L. S. Verduyn, S. M. V. Lunel, Introduction to functional differential equations, Vol. 99, Springer Science & Business Media, 1993.

[15] W. Michiels, S.-I. Niculescu, Stability, control, and computation for time-delay systems: An eigenvalue-based approach, 2nd Edition, Vol. 27 of Advances in Design and Control, Society for Industrial and Applied Mathematics (SIAM), Philadelphia, PA, 2014.

[16] G. Stépán, Retarded dynamical systems: stability and characteristic functions, Longman Scientific & Technical, 1989.

[17] L. Mirkin, On dead-time compensation in repetitive control, IEEE Control Systems Letters 4 (4) (2020) 791–796.

[18] T. Inoue, Practical repetitive control system design, in: 29th IEEE Conference on Decision and Control, IEEE, 1990, pp. 1673–1678.

[19] W. S. Chang, I. H. Suh, T. W. Kim, Analysis and design of two types of digital repetitive control systems, Automatica 31 (5) (1995) 741–746.

[20] M. Steinbuch, Repetitive control for systems with uncertain period-time, Automatica 38 (12) (2002) 2103–2109.

[21] G. Pipeleers, B. Demeulenaere, J. De Schutter, J. Swevers, Robust high-order repetitive control: optimal performance trade-offs, Automatica 44 (10) (2008) 2628–2634.

[22] M. Steinbuch, S. Weiland, T. Singh, Design of noise and period-time robust high-order repetitive control, with application to optical storage, Automatica 43 (12) (2007) 2086–2095.

[23] G. Pipeleers, B. Demeulenaere, J. Swevers, Optimal linear controller design for periodic inputs, Vol. 394, Springer, 2009.

[24] L. Güvenç, Stability and performance robustness analysis of repetitive control systems using structured singular values, Journal of Dynamic Systems, Measurement, and Control (1996).

[25] J.-H. Moon, M.-N. Lee, M. J. Chung, Repetitive control for the track-following servo system of an optical disk drive, IEEE transactions on control systems technology 6 (5) (1998) 663–670.

[26] T.-Y. Doh, M. J. Chung, Repetitive control design for linear systems with time-varying uncertainties, IEE Proceedings-Control Theory and Applications 150 (4) (2003) 427–432.

[27] K. Omura, H. Ujikawa, O. Kaneko, Y. Okano, S. Yamamoto, H. Imanari, T. Horikawa, Attenuation of roll eccentric disturbance by modified repetitive controllers for steel strip process with transport time delay, IFAC-PapersOnLine 48 (17) (2015) 131–136.

[28] R.-J. Liu, G.-P. Liu, M. Wu, J. She, Z.-Y. Nie, Robust disturbance rejection in modified repetitive control system, Systems & Control Letters 70 (2014) 100–108.

[29] K. Cai, Z. Deng, C. Peng, K. Li, Suppression of harmonic vibration in magnetically suspended centrifugal compressor using zero-phase odd-harmonic repetitive controller, IEEE Transactions on Industrial Electronics 67 (9) (2019) 7789–7797.

[30] X. Sun, Z. Jin, L. Chen, Z. Yang, Disturbance rejection based on iterative learning control with extended state observer for a four-degree-of-freedom hybrid magnetic bearing system, Mechanical Systems and Signal Processing 153 (2021) 107465.

[31] D. Astolfi, S. Marx, N. van de Wouw, Repetitive control design based on forwarding for nonlinear minimum-phase systems, Automatica 129 (2021) 109671.

[32] T.-C. Tsao, Y.-X. Qian and, M. Nemani, Repetitive control for asymptotic tracking of periodic signals with an unknown period, J. Dyn. Sys., Meas., Control 122 (2) (2000) 364–369.

[33] G. Hillerstrom, Adaptive suppression of vibrations-a repetitive control approach, IEEE Transactions on Control Systems Technology 4 (1) (1996) 72–78.

[34] J. Chen, J. Li, N. Yang, Globally repetitive learning consensus control of unknown nonlinear multi-agent systems with uncertain time-varying parameters, Applied Mathematical Modelling 89 (2021) 348–362.

[35] H. Liang, L. Chen, Y. Pan, H.-K. Lam, Fuzzy-based robust precision consensus tracking for uncertain networked systems with cooperative-antagonistic interactions, IEEE Transactions on Fuzzy Systems (2022).

[36] L. Cao, Y. Pan, H. Liang, T. Huang, Observer-based dynamic event-triggered control for multiagent systems with time-varying delay, IEEE Transactions on Cybernetics (2022).

[37] M. Goubej, T. Vyhlídal, M. Schlegel, Frequency weighted h2 optimization of multi-mode input shaper, Automatica 121 (2020) 109202.

[38] T. Vyhlídal, M. Hromčík, V. Kučera, M. Anderle, On feedback architectures with zero-vibration signal shapers, IEEE Transactions on Automatic control 61 (8) (2015) 2049–2064.

[39] T. Vyhlídal, M. Hromčík, Parameterization of input shapers with delays of various distribution, Automatica 59 (2015) 256–263.

[40] T. Vyhlídal, V. Kučera, M. Hromčík, Signal shaper with a distributed delay: Spectral analysis and design, Automatica 49 (11) (2013) 3484–3489.

[41] T. Vyhlídal, D. Pilbauer, B. Alikoç, W. Michiels, Analysis and design aspects of delayed resonator absorber with position, velocity or acceleration feedback, Journal of Sound and Vibration 459 (2019) 114831.

[42] D. Pilbauer, T. Vyhlídal, W. Michiels, Optimized design of robust resonator with distributed time-delay, Journal of Sound and Vibration 443 (2019) 576–590.

[43] D. Pilbauer, T. Vyhlídal, N. Olgac, Delayed resonator with distributed delay in acceleration feedback—design and experimental verification, IEEE/ASME Transactions on Mechatronics 21 (4) (2016) 2120–2131.

[44] C. E. Garcia, M. Morari, Internal model control. a unifying review and some new results, Industrial & Engineering Chemistry Process Design and Development 21 (2) (1982) 308–323.

[45] Y.-S. Lu, Internal model control of lightly damped systems subject to periodic exogenous signals, IEEE Transactions on Control Systems Technology 18 (3) (2009) 699–704.

[46] T. Vyhlídal, P. Zítek, Control system design based on a universal first order model with time delays, Acta Polytechnica 41 (4-5) (2001).

[47] P. Zítek, J. Bušek, T. Vyhlídal, Anti-windup conditioning for actuator saturation in internal model control with delays, in: Low-Complexity Controllers for Time-Delay Systems, Springer, 2014, pp. 31–45.

[48] C. Grimholt, S. Skogestad, Optimal pi and pid control of first-order plus delay processes and evaluation of the original and improved simc rules, Journal of Process Control 70 (2018) 36–46.

[49] L. Sun, W. Xue, D. Li, H. Zhu, Z.-g. Su, Quantitative tuning of active disturbance rejection controller for foptd model with application to power plant control, IEEE Transactions on Industrial Electronics 69 (1) (2021) 805–815.

[50] S. Skogestad, I. Postlethwaite, Multivariable feedback control: analysis and design, john Wiley & sons, 2005.

[51] C.-I. Morărescu, S.-I. Niculescu, K. Gu, On the geometry of stability regions of smith predictors subject to delay uncertainty, IMA Journal of Mathematical Control and Information 24 (3) (2007) 411–423.

[52] S. Skogestad, I. Postlethwaite, Multivariable feedback control: analysis and design, Vol. 2, Citeseer, 2007.

[53] W. Michiels, S. Gumussoy, Computation of h-infinity norms for time-delay systems, TW Reports (2009).

[54] S. Gumussoy, W. Michiels, Computation of extremum singular values and the strong h-infinity norm of siso time-delay systems, Automatica 54 (2015) 266–271.

[55] S. Gumussoy, W. Michiels, Fixed-order h-infinity control for interconnected systems using delay differential algebraic equations, SIAM Journal on Control and Optimization 49 (5) (2011) 2212–2238.

[56] M. Overton, Hanso: a hybrid algorithm for nonsmooth optimization, Available from cs. nyu. edu/overton/software/hanso (2009).

[57] F. E. Curtis, T. Mitchell, M. L. Overton, A bfgs-sqp method for nonsmooth, nonconvex, constrained optimization and its evaluation using relative minimization profiles, Optimization Methods and Software 32 (1) (2017) 148–181.

[58] W. Michiels, S.-I. Niculescu, Stability, control, and computation for time-delay systems: an eigenvalue-based approach, SIAM, 2014.

[59] J. Chen, Sensitivity integral relations and design trade-offs in linear multivariable feedback systems, IEEE Transactions on Automatic Control 40 (10) (1995) 1700–1716.